



Portable GNSS Software-Defined Receiver Based on ADALM-Pluto SDR

EEE493 Industrial Design Project I Committee Meeting 1 Report

Electrical and Electronics Engineering Department

Group Members: Yiğit Kağan Öztürk, Emre Kurt, Emre Şaş,
Gökay Solak, Awais Ahmad Awan, Berfin Lara Bilgen

Academic Mentor: Asst. Prof. Özlem Tuğfe Demir

Company Mentor: Ahmet Mekih Gedikli

Teaching Assistant: Batuhan Uykulu

14.11.2025



VisionX Technology develops AI-powered satellite intelligence systems, including onboard flight computers, smart payload controllers, and edge computing solutions for space missions. The company works across LEO, GEO, and deep-space mission domains, offering expertise in autonomous payload processing, subsystem interface control (SpaceWire, CAN, RS-422/485), and real-time health monitoring and fault resilience.

TABLE OF CONTENTS

ABSTRACT.....	4
LIST OF FIGURES.....	5
LIST OF TABLES.....	6
1. MOTIVATION AND NOVELTY.....	1
2. REQUIREMENTS.....	2
2.1 Functional Requirements:.....	3
2.1.1 Hardware Functional Requirements.....	3
2.1.2 Software Functional Requirements.....	3
2.1.3 GNSS Signal Algorithms Functional Requirements.....	3
2.1.4 GUI Functional Requirements.....	4
2.2 Non-Functional Requirements/Constraints:.....	4
3. METHODS AND IMPLEMENTATION DETAILS.....	5
3.1 Work Breakdown Structure and Project Plan.....	5
3.1.1 Work Packages.....	6
3.1.2 Milestones.....	7
3.2 Methods and Progress.....	7
3.2.1 Methods and Tools.....	7
3.2.1.1 Hardware Setup and System Configuration.....	7
3.2.1.1.A Active GNSS Antenna (u-blox ANN-MB2-00) [7].....	8
3.2.1.1.B Bias-Tee (Mini-Circuits ZFBT-4R2G+) [8].....	9
3.2.1.1.C DC Block (Mini-Circuits BLK-89-S+) [9].....	10
3.2.1.1.D External Temperature-Compensated Crystal Oscillator (Epson TG2520SMN) [10].....	10
3.2.1.1.E ADALM-Pluto SDR (AD9363 + Zynq-7010 SoC) [3].....	11
3.2.1.1.F Clock Integration Method.....	12
3.2.1.1.G Overall Hardware Architecture.....	13
3.2.1.1.H Hardware focused Risks and Mitigation.....	13
3.2.1.2 Acquisition Method in GNSS Signal Processing.....	14
3.2.1.2.A Signal Reception and Sampling.....	15
3.2.1.2.B Delay–Doppler Search Space Formation.....	15
3.2.1.2.C FFT-Based Acquisition in the Frequency Domain.....	16
3.2.1.2.D Optimization Techniques (Comb, Multi-Frequency).....	17
3.2.1.2.E Detection and Decision.....	18
3.2.1.3 Tracking Method in GNSS Signal Processing.....	19
3.2.1.4 Telemetry Decoding and Data Processing.....	19
3.2.1.5 PVT Computation.....	19
3.2.1.6 GUI Design and System Integration.....	20
3.2.2 Progress and the current state.....	21

4. DETAILED EQUIPMENT LIST.....	22
5. REFERENCES.....	23

ABSTRACT

The Portable GNSS Software-Defined Receiver Based on ADALM-Pluto SDR project aims to create a hardware and software integrated GNSS signal processing block that is modular, flexible and low cost. The project aims to achieve acquisition of 6 satellites in 20s and generate position, velocity, and time solutions based on the received satellite signal. In order to achieve it, Adalm-Pluto SDR will be used as an RF receiver front end which receives the L1, K2 band signals and transmits I/Q (In-phase and Quadrature) baseband signal to the host computer for further signal processing. The host PC should run GNU Radio/GNSS SDR to handle signal acquisition, tracking, telemetry decoding and finally PVT solution generation. The aim is to have a horizontal error of at most 20 meters. In terms of development and testing of the system, individual signal processing stages are aimed to be simulated in MATLAB/Simulink and GNU Radio/GNSS SDR environments with prerecorded data. After validation over prerecorded data, it is aimed to be tested on Adalm-Pluto SDR in real life environments. In terms of expected results, it is aimed to ensure that the receiver and individual algorithms satisfy the performance metrics and are organized in a modular/flexible manner.

LIST OF FIGURES

Figure 1: Some global GNSS satellite organizations	1
Figure 2: Work Breakdown Structure.	5
Figure 3: Project's Gantt Chart.	7
Figure 4: u-blox ANN-MB2-00	8
Figure 5: Simplified ANN-MB2-00 block diagram	9
Figure 6: Mini-Circuits ZFBT-4R2G+ and the circuit inside it	9
Figure 7: Mini-Circuits BLK-89-S+	10
Figure 8: ADALM-Pluto SDR Front-End Device	11
Figure 9: Simplified block diagram of a generic radio frequency front-end.	12
Figure 10: Pin Layout (AD9363 (Rev. C))	13
Figure 11: GNSS front-end Integration	13
Figure 12: Two-Dimensional Search Space of Delay and Doppler Frequency	15
Figure 13: FFT-Based Circular Correlation Block Diagram	17
Figure 14: PCPS algorithm simulations on MATLAB with pre-recorded data.	21
Figure 15: Generated PCPS plot and PSD analysis of pre-recorded data	21
Figure 16: Generated PVT Solutions using GNSS SDR.	21
Figure 17: Progress Up to now (14.11.2025) on Gantt Chart	22

LIST OF TABLES

Table 1: Hardware Functional Requirements	3
Table 2: Software Functional Requirements	3
Table 3: Algorithm Functional Requirements	3
Table 4: GUI Requirements	4
Table 5: Non-functional Requirements	4
Table 6 :Technical Specifications of u-blox ANN-MB2-00	9
Table 7: Technical Specifications of Mini-Circuits ZFBT-4R2G+	10
Table 8: Technical Specifications of ADALM-Pluto SDR and Epson TG2520SMN	12
Table 9: Hardware focused Risks, Impacts and Mitigation solutions	14
Table 10 : Acquisition focused Risks, Impacts and Mitigation solutions	18
Table 11: Tracking focused Risks, Impacts and Mitigation solutions	19
Table 12 : Telemetry decoding focused Risks, Impacts and Mitigation solutions	19
Table 13 : PVT algorithm focused Risks, Impacts and Mitigation solutions	20
Table 14 : GUI focused Risks, Impacts and Mitigation solutions	20
Table 15: Detailed equipment list and costs	22

1. MOTIVATION AND NOVELTY

The Portable GNSS Software-Defined Receiver Based on ADALM-Pluto SDR project mainly focuses on developing a low cost, hardware and software integrated, modular GNSS signal processing block that can be updated and modulated based on possible future applications.

The core expectations on the project can be listed as the software and hardware infrastructure being flexible, fully open source and with a considerably low cost. Since the available stand-alone GNSS signal processing products on the market are not promising, these three expectations simultaneously are what the project aims to provide in a GNSS signal processing system that can perform signal processing required for GNSS applications in a modular manner and with a considerably lower cost.

The project comes out as being crucial in terms of contributing to the national expertise on space missions and technologies. The main operating satellite systems in the global scale can be exemplified as GALILEO which is operated and funded by European Union, GPS which is operated and funded by USA, GLONASS established by USSR and operated and funded by Russia, BEIDOU operated and funded by China, QZSS operated and funded by Japan and many more [1].



Figure 1: Some global GNSS satellite organizations [1].

Regarding the GNSS space applications, the main providers can be observed as global actors, countries, and organizations. Therefore, from a national perspective contributing to national space expertise can be regarded as a crucial aspect of Portable GNSS Software-Defined Receiver Based on ADALM-Pluto SDR project.

Moreover, from the market's, developers' and GNSS enthusiasts' perspective, the project aims to provide the community with an operational GNSS signal processing hardware and software block that has portability, modularity, flexibility features with a considerably low cost aiming to enhance the development of efficient and accessible GNSS signal processing systems.

In the market, there are commercial and research-based GNSS receivers and signal processing blocks. To exemplify some commercial products, manufacturers such as Qualcomm, u-blox, and Septentrio provide GNSS receiver and signal processing modules. Closed source (with embedded firmware), algorithms and data access are limited. They deliver high accuracy but are restricted in terms of

customizability and cost. To exemplify, mosaic-go X5 GNSS module receiver evaluation kit including only the signal processing block costing 1300 USD comparing with the expected cost of Portable GNSS Software-Defined Receiver Based on ADALM-Pluto SDR as 450 USD with all hardware and software packs, comes out as considerably expensive and having limited modularity and accessibility [2]. Additionally, research-oriented products on the market such as USRP Ettus, bladeRF, and HackRF are widely used in GNSS research. Although they are highly flexible, they are considerably expensive, for example USRP B210 costs 1700 USD [3]. Hence, the novelty of the Portable GNSS Software-Defined Receiver Based on ADALM-Pluto SDR project comes out as promising modularity, flexibility and efficiency with a considerably low cost simultaneously.

A preliminary patent search shows that some sub parts of the Portable GNSS Software Defined Receiver Based on ADALM-Pluto SDR are already patented by different solutions. Therefore, receiving a patent on the project alone is unlikely. To exemplify, there are patented real-time GNSS software receivers [4], [5] and low-power, low-cost GNSS receiver architectures [6]. Additionally, some open-source GNSS-SDR frameworks already support ADALM-Pluto as a front end, indicating that the combination of Pluto SDR and GNSS signal processing may not be regarded as enough for receiving a patent.

SDR based receiver structures support high modularity and flexibility, where in space missions the modularity and software-based improvement instead of direct hardware-based interference is more preferable. Hence, software defined GNSS receivers are promising in terms of space missions, on board satellite computers and even ground receiver terminals. Regarding these aspects VisionX Technology, whose main occupation is in development of satellite on board flight computers, comes out as being eager to integrate SDR based GNSS products into their systems. Hence, Portable GNSS Software-Defined Receiver Based on ADALM-Pluto SDR project's developed software and hardware infrastructure with probable research and development phase is aimed to be integrated with preexisting systems and expected to be integrated in ongoing developments for the satellite on board computer for Gezgin 1 which is planned to be launched in 2028. Additionally, the developed software and hardware infrastructure and know-how is aimed to be used for real-time positioning and time synchronization for CubeSat and microsatellite platforms in future. Consequently, VisionX Technology aims to gain infrastructure and know-how on the SDR based GNSS signal processing blocks at the end of the project to develop SDR based subsystems for space missions.

2. REQUIREMENTS

The purpose of this system is to develop a software-defined GNSS receiver capable of acquiring, tracking, and computing position velocity and time (PVT) solutions from L1 and L2 band GNSS signals using a single SDR device for RF front end. The SDR device serves as an RF front-end connected to a host PC running Ubuntu 22.04. The system will operate with the open-source GNU Radio and GNSS-SDR frameworks. The host PC runs GNU Radio and GNSS-SDR, which perform acquisition, tracking, and PVT calculation.

The system should be able to:

- I. Receive and digitize and transmit GNSS frequency bands (GPS L1 and GPS L2).
- II. Acquire and track signals from at least six visible satellites.
- III. Compute position solutions within 20s (cold start).
- IV. Achieve \leq 20m radial position accuracy in open-sky conditions.

2.1 Functional Requirements:

2.1.1 Hardware Functional Requirements

Table 1: Hardware Functional Requirements

ID	Requirement	Requirement Statement
HW-FR-1	Data Transmission Requirement.	Data transmission rate $>$ 4 MSPS.
HW-FR-2	Local Oscillator Stability Requirement.	The internal LO should maintain frequency stability within ± 1 ppm over 0–40 °C.

2.1.2 Software Functional Requirements

Table 2: Software Functional Requirements

ID	Requirement	Requirement Statement
SW-FR-1	SDR Configuration Control	The software shall control RX channels of the SDR device, including frequency, gain, and sample-rate configuration.
SW-FR-2	Modular Architecture	Each GNSS-SDR block (acquisition, tracking, navigation) shall be modular and replaceable.

2.1.3 GNSS Signal Algorithms Functional Requirements

Table 3: Algorithm Functional Requirements

ID	Requirement	Requirement Statement
ACQFR-1	Signal Detection	The acquisition module shall detect and identify signals from at least six GNSS satellites within 20 seconds after startup.
TRKFR-1	Lock Maintenance	Tracking module maintains carrier and code lock for at least 6 satellites.

PVTFR-1	Position Accuracy	Navigation module shall compute 3D position and velocity once per second with $\leq 20\text{m}$ RMS horizontal error under open-sky conditions.
PVTFR-2	Data Logging	The system shall store PVT solutions, acquired satellites, and tracking data with synchronized timestamps.

2.1.4 GUI Functional Requirements

Table 4: GUI Requirements

ID	Requirement	Requirement Statement
GUI-R-1	CNR Display	The GUI shall display the estimated C/N_0 (CNR).
GUI-R-2	Satellite Constellation View	The user interface shall display real-time satellite constellation tracking within 1s of update.
GUI-R-3	Satellite Count Indicator	The GUI shall exhibit the acquired number of satellites.
GUI-R-4	Position Display	The GUI will show the computed position updated every 1s.

2.2 Non-Functional Requirements/Constraints:

Table 5: Non-functional Requirements

ID	Requirement	Requirement Statement
NFR-1	Maximum allowable cost	Less than 1000 USD.
NFR-2	Maximum allowable size, weight	None.
NFR-3	Power requirement/constraint	Not Applicable
NFR-4	Environmental operating conditions and other issues	The receiver shall operate under -10°C to $+50^{\circ}\text{C}$, 0–85 % RH, and resist mild vibration and sunlight exposure during outdoor field tests.
NFR-5	Safety issues	The design shall ensure electrical and RF safety, including proper grounding, ESD protection, and safe antenna voltage biasing (< 5 V).

NFR-6	Health constraints and requirements	None
NFR-7	Global, cultural, and social factors	Global applicability and open-source collaboration
NFR-8	References related to the standards that the product will be compatible with	EMC Directive 2014/30/EU, RoHS 2 Directive 2011/65/EU, IEC 60950-1:2005

3. METHODS AND IMPLEMENTATION DETAILS

In this section, the project's main work packages and plans are explained. The milestones related to the work packages are shown. The relations between requirements of the project, milestones, and work packages are examined.

3.1 Work Breakdown Structure and Project Plan

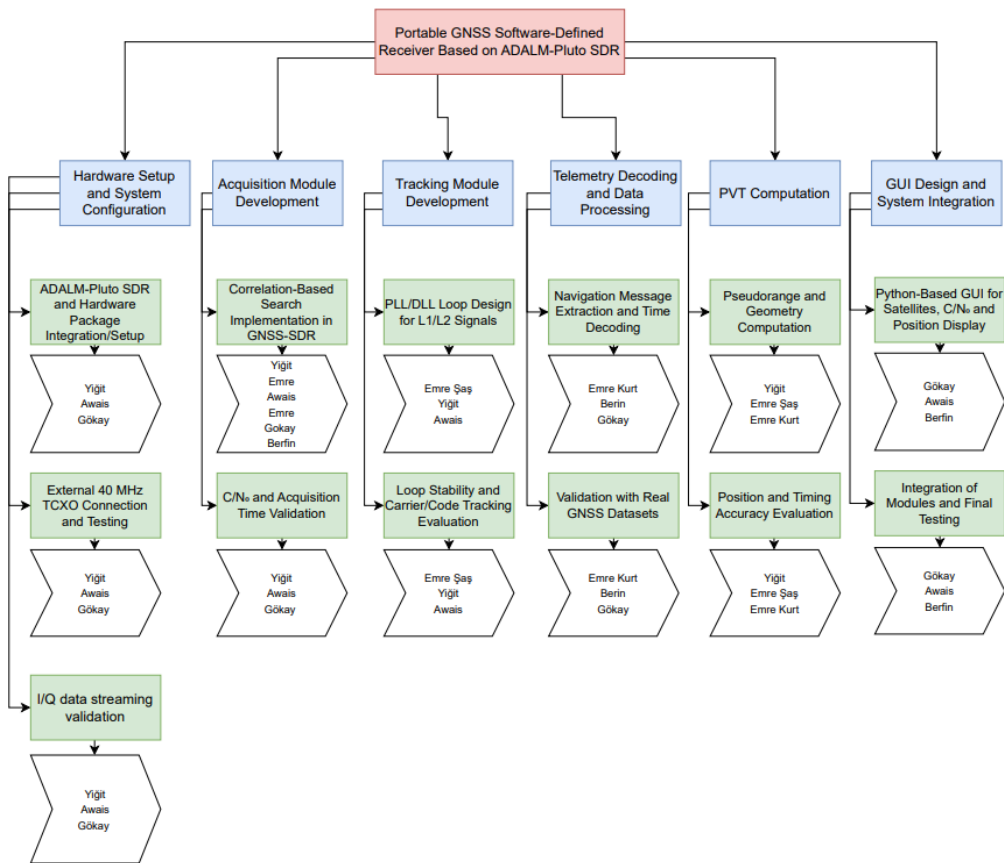


Figure 2: Work Breakdown Structure.

3.1.1 Work Packages

The project is organized into six main work packages, each representing a core functional block of the GNSS software-defined receiver. These work packages allow parallel development of hardware, signal-processing algorithms, and software modules while ensuring that all components can later be integrated into a unified system.

WP1 – Hardware Setup and System Configuration: This work package includes the selection and integration of all RF front-end components such as the active GNSS antenna, bias-tee, DC block, and ADALM-Pluto SDR. It also covers the external TCXO clock integration, SDR parameter configuration (frequency, gain, sampling rate), and initial I/Q data capture tests. WP1 establishes the physical and digital foundation required for all subsequent work packages.

WP2 – Acquisition Module Development: WP2 focuses on the design and implementation of GNSS satellite acquisition algorithms using GNSS-SDR. Tasks include delay-Doppler search implementation, FFT-based correlation, thresholding logic, and verification of acquisition time and C/N₀ performance using prerecorded datasets. This work package ensures the system can correctly identify visible satellites and provide initial signal parameters.

WP3 – Tracking Module Development: This work package involves implementing DLL, FLL, and PLL tracking loops to maintain continuous synchronization with acquired satellites. Activities include loop filter configuration, carrier/code tracking validation, stability checks under varying signal conditions, and real-time tuning for optimal lock performance.

WP4 – Telemetry Decoding and Data Processing: WP4 covers the extraction of navigation message bits from the tracked signals. Tasks include frame synchronization, parity checking, ephemeris decoding, and preparing cleaned navigation data for the PVT module. This package ensures accurate observables and timing data are available for position computation.

WP5 – PVT Computation: This work package focuses on computing the receiver's position, velocity, and time using decoded satellite data. Tasks include pseudorange calculation, least-squares position estimation, clock bias correction, and verification of horizontal error performance against expected metrics.

WP6 – GUI Design and System Integration: WP6 includes the development of a lightweight Python-based GUI to visualize system outputs such as C/N₀, satellite count, constellation view, and 1 Hz position updates. It also covers the integration of all work packages into a seamless end-to-end receiver pipeline. This is the final phase and will be completed after acquisition, tracking, and PVT modules are fully validated.

3.1.2 Milestones

The figure below represents the Work Division Table (WDT) and project timeline for the GNSS-SDR receiver development project. Each main task group (*GNSS SDR Environment Set Up, Acquisition Module Development, Tracking Module Development, Telemetry Decoding and Data Processing, PVT Computation, GUI Design and System Integration*) is divided into detailed subtasks to clarify the workflow.

The Gantt-style timeline shows the planned start and end weeks across the academic year, covering Fall, the semester break, and Spring. This visual layout helps track progress, coordinate parallel work, and align module-level development with milestone deadlines such as CM1, L1–L3, and CM2. The milestones success criteria can be explained as for each regarding work package satisfying the requirements; Namely HW-FR-1 and 2, SW-FR-1 and 2, ACQFR-1, TRKFR-1, PVTFR-1 and 2, GUI-R-1 to GUI-R-4.

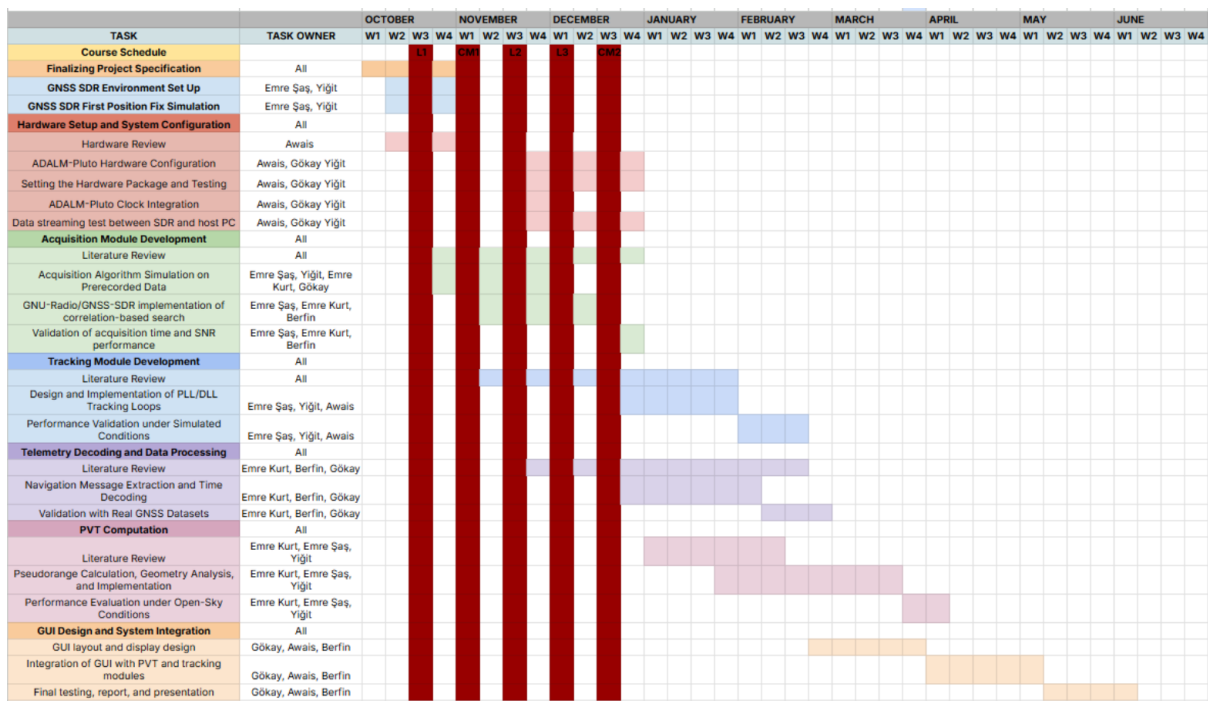


Figure 3: Project's Gantt Chart.

3.2 Methods and Progress

In this section, the methods and tools relevant to the project's work packages and the group's progress will be discussed.

3.2.1 Methods and Tools

3.2.1.1 Hardware Setup and System Configuration

The hardware infrastructure of the Portable GNSS Software-Defined Receiver is designed to create a stable, low-noise, and modular RF front-end capable of reliably receiving GPS L1 and L2 signals and streaming digitized I/Q samples to the host PC for processing. The chosen hardware elements including active GNSS antenna, bias-tee, DC block, ADALM-Pluto SDR, and an external TCXO, together form a coherent reception chain that meets the functional requirements HW-FR-1 (4 MSPS streaming) and HW-FR-2 (± 1 ppm LO stability). In this context, the datasheets

of the possible equipment set were studied and working principles were understood and explained.

3.2.1.1.A Active GNSS Antenna (u-blox ANN-MB2-00) [7]



Figure 4: u-blox ANN-MB2-00

The ANN-MB2-00 is the primary RF sensor of the system. GNSS signals arriving at Earth have extremely low power levels (typically -130 to -140 dBm). To make these signals detectable by the SDR, the antenna integrates the following internal functions which are also summarized in figure 5:

- i. **Ceramic Patch Radiator (RHCP):** It is designed for Right-Hand Circular Polarization to match satellite transmission, improve sky visibility, and reduce multipath from the ground.
- ii. **SAW Band-Pass Filters (L1/L2/L5 Bands):** Narrowband filters suppress out-of-band interference (LTE, Wi-Fi, ISM bands), reducing the effective noise bandwidth.
- iii. **Low-Noise Amplifier (LNA):** The LNA provides ~ 30 dB gain with 2.5–3 dB noise figure, boosting the weak GNSS signals before cable losses (~ 5 –6 dB) and thus dominates the receiver noise figure. The reason amplification is done *inside the antenna* rather than in the SDR is that once the signal travels through the long coaxial cable, losses would reduce it below the receiver's noise floor. By amplifying first, the LNA effectively “raises” the signal above the noise introduced later by the cable and SDR input. Mathematically, the overall noise figure F_{total} of cascaded stages is given by the Friis formula:

$$F_{\text{total}} = F_1 + (F_2 - 1)/G_1 + (F_3 - 1)/(G_1 G_2) + \dots$$

- iv. **Integrated Bias Network:** It accepts 3–5 V DC through the coaxial cable to power the LNA.

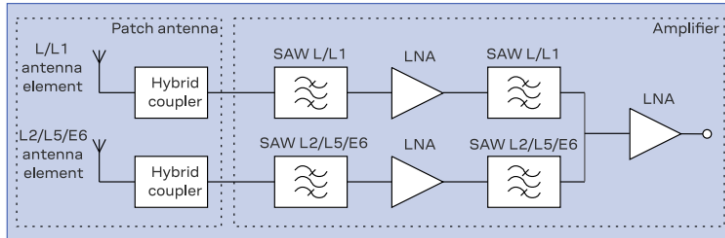


Figure 5: Simplified ANN-MB2-00 block diagram

The following table specifies the technical performance in relevance to our project:

Table 6: Technical Specifications of u-blox ANN-MB2-00

Parameter	GPS L1 Band	L5/L2/B3/E6 Band	In context of our project
Frequency range	1535–1602 MHz	1166–1285 MHz	Covers required GPS L1 & L2 bands.
Patch gain	$\approx +5$ dBic	$\approx +4.5$ dBic	Directional gain toward sky; reduces ground noise.
LNA gain	31 ± 3 dB	31.5 ± 3 dB	Amplifies the microvolt-level signals to millivolt range.
Noise figure	3 dB	2.5 dB	Adds minimal noise, crucial for weak GNSS signals.
Output VSWR	$\approx 2:1$	$\approx 2:1$	Good impedance match to 50 Ω coax.
Cable insertion loss	6.5 dB	5.5 dB	Loss of 5 m RG-174 cable compensated by LNA gain.
Total system gain	≈ 23 dB	≈ 23 dB	What arrives at SDR input.

3.2.1.1.B Bias-Tee (Mini-Circuits ZFBT-4R2G+) [8]

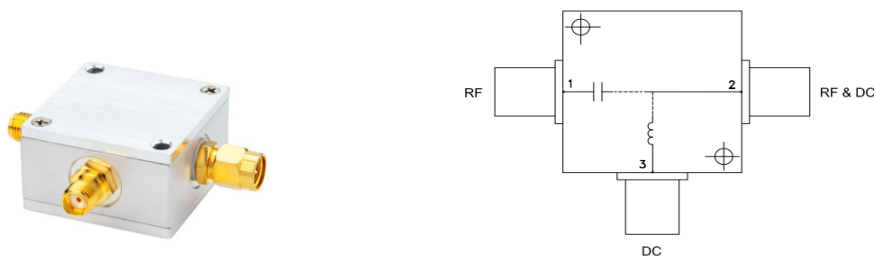


Figure 6: Mini-Circuits ZFBT-4R2G+ and the circuit inside it.

Since the ADALM-Pluto does not provide bias voltage to power the antenna LNA, a bias-tee is inserted between the antenna and the SDR. The internal working principle is given in Figure 6. The Inductor Arm allows passing DC while presenting high impedance to RF signal while Capacitor Arm passes RF while blocking DC. This ensures the antenna receives power but the SDR input remains fully DC-isolated. Following table summarizes the Bias-T's technical specifications:

Table 7: Technical Specifications of Mini-Circuits ZFBT-4R2G+

Parameter	Description
DC Injection	Supplies 3–5 V to the antenna along the coaxial line
RF Passband	10 MHz–4.2 GHz, covering all GNSS bands
Isolation	~40 dB isolation between DC path and RF path which prevents unwanted coupling between the supply and the signal.
Low Loss	<0.7 dB insertion loss at L1/L2

3.2.1.1.C DC Block (Mini-Circuits BLK-89-S+) [9]

In our GNSS receiver chain, a DC block is inserted between the bias-tee and the Pluto SDR to protect the RF input stage against potential DC leakage or voltage spikes. The DC block uses a high-quality series capacitor to provide complete DC isolation while maintaining RF transparency from 0.1–8000 MHz and introducing negligible insertion loss (<0.1 dB).



Figure 7: Mini-Circuits BLK-89-S+

This prevents accidental damage from bias-tee power or wiring mistakes and ensures long-term safety during outdoor testing (aligned with NFR-5).

3.2.1.1.D External Temperature-Compensated Crystal Oscillator (Epson TG2520SMN) [10]

(Explained in the subsequent section)

3.2.1.1.E ADALM-Pluto SDR (AD9363 + Zynq-7010 SoC) [3]

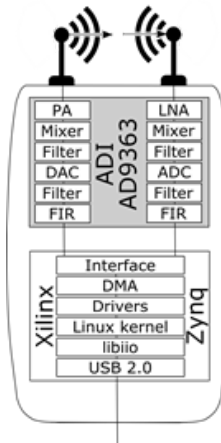


Figure 8: ADALM-Pluto SDR Front-End Device

The ADALM-Pluto SDR functions as the primary RF front-end and digitization platform of the GNSS receiver. Based on the AD9363 RF Agile Transceiver and Zynq-7010 SoC, Pluto performs RF tuning, analog filtering, automatic gain control, quadrature mixing, and 12-bit I/Q digitization required for GNSS L1/L2 processing. After downconversion, the Pluto streams continuous baseband I/Q samples to the host PC through USB 2.0, where acquisition, tracking, telemetry decoding, and PVT computations are executed using GNU Radio and GNSS-SDR. Full software control over the SDR, including center frequency, sampling rate, RF gain, and digital filter bandwidth, supports the modular structure described in SW-FR-1 and ensures that the hardware front-end is fully configurable for different GNSS signals and test conditions. Figure 10 illustrates this workflow in a block diagram.

One thing to note is that for GNSS applications, frequency stability is a critical factor. Pluto's default 40 MHz crystal exhibits ± 25 ppm stability, leading to local oscillator drift, carrier tracking instability, and degraded Doppler accuracy, especially noticeable in weak-signal environments. To ensure compliance with HW-FR-2 (LO stability $\leq \pm 1$ ppm), the SDR is upgraded with an external Epson TG2520SMN 40 MHz Temperature-Compensated Crystal Oscillator (TCXO). The TG2520SMN provides ± 0.5 ppm stability over a wide thermal range, as well as significantly lower phase noise. This reduces frequency error at the L1 band to approximately ± 787 Hz, improving PLL/DLL stability, extending coherent integration times, and enabling consistent multi-satellite tracking under real operating conditions.

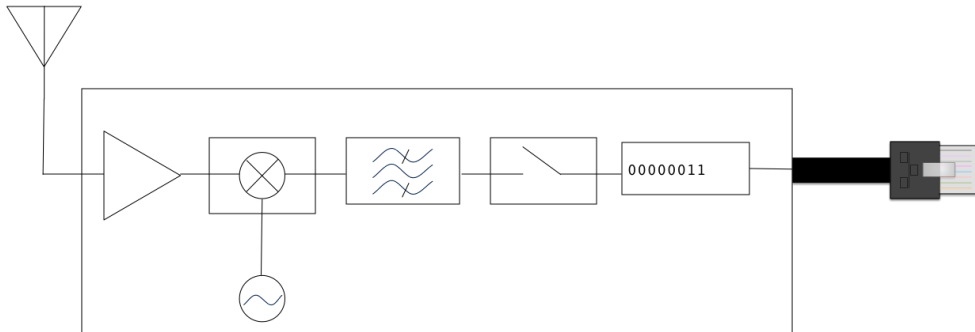


Figure 9: Simplified block diagram of a generic radio frequency front-end.

Following table summarizes the technical specification for both ADALM-Pluto SDR and External TCXO:

Table 8: Technical Specifications of ADALM-Pluto SDR and Epson TG2520SMN

Parameter	Specification	Relevance to GNSS Receiver
Frequency Range	325 MHz – 3.8 GHz	Covers GPS L1 (1575.42 MHz) & L2 (1227.60 MHz)
ADC Resolution	12-bit I/Q	Adequate for weak GNSS signal dynamic range
Maximum Sample Rate	61.44 MSPS (Effective 4–5 MSPS via USB 2.0)	Meets real-time streaming requirement (HW-FR-1)
RF Gain Control	–10 dB to +70 dB	Full software control (SW-FR-1)
Default Clock Source	Internal 40 MHz XO (± 25 ppm)	Insufficient stability for GNSS tracking
Upgraded Clock Source	Epson TG2520SMN TCXO (40 MHz)	Provides ± 0.5 ppm precision
TCXO Stability	± 0.5 ppm (-40°C to $+85^\circ\text{C}$)	Meets HW-FR-2 requirement
TCXO Phase Noise	-161 dBc/Hz @ 100 kHz offset	Enables long coherent integrations
TCXO Power Consumption	$\sim 2 \text{ mA}$ @ 3.3 V	Suitable for continuous operation

3.2.1.1.F Clock Integration Method

The integration of the external TCXO into the Pluto SDR is performed using the supported reference-clock override path of the AD9363 transceiver. The AD9363 allows its internal synthesizers and PLLs to be driven either by the onboard crystal or by an externally supplied 40 MHz reference fed directly into the XTALN input pin. In this project, the external TG2520SMN TCXO is connected to the SDR through its reference-clock port, allowing Pluto to operate entirely based on the TCXO's stable frequency source. Figure 11 shows the pin layout of AD9363 (Revision C) and relevant pin for TCXO integration.

This integration approach does not require destructive hardware modification and as a result, the SDR benefits from a high-stability, low-phase-noise master clock, improving Doppler estimation, reducing carrier phase jitter, and ensuring the timing accuracy needed for reliable GNSS acquisition and tracking.

Pin Layout (AD9363 Rev. C)

	1	2	3	4	5	6	7	8	9	10	11	12
A	RX2A_N	RX2A_P	DNC	VSSA	TX_MON2	VSSA	TX2A_N	TX2A_P	TX2B_N	TX2B_P	VDDA1P1_TX_VCO	VSSA
B	VSSA	VSSA	AUXDAC1	GPO_3	GPO_2	GPO_1	GPO_0	VDD_GPO	VDDA1P3_TX_LO	VDDA1P3_TX_VCO_LDO	VDDA1P3_TX_VCO_LDO_OUT	VSSA
C	RX2C_P	VSSA	AUXDAC2	TEST/ENABLE	CTRLL_IN0	CTRLL_IN1	VSSA	VSSA	VSSA	VSSA	VSSA	VSSA
D	RX2D_N	VDDA1P3_RX_RF	VDDA1P3_RX_RF	CTRLL_OUT0	CTRLL_IN3	CTRLL_IN2	P0_D9/TX_D4_P	P0_D7/TX_D3_P	P0_D5/TX_D2_P	P0_D3/TX_D1_P	P0_D1/TX_D0_P	VSSD
E	RX2B_P	VDDA1P3_RX_LO	VDDA1P3_RX_LO BUFFER	CTRLL_OUT1	CTRLL_OUT2	CTRLL_OUT3	P0_D11/TX_D5_P	P0_D8/TX_D4_N	P0_D6/TX_D3_N	P0_D4/TX_D2_N	P0_D2/TX_D1_N	P0_D0/TX_D0_N
F	RX2B_N	VDDA1P3_RX_VCO_LDO	VSSA	CTRLL_OUT6	CTRLL_OUT5	CTRLL_OUT4	VSSD	P0_D10/TX_D5_N	VSSD	FB_CLK_P	VSSD	VDD01P3_DIG
G	VSSA	RX_VCO_LDO_OUT	VDDA1P1_RX_VCO	CTRLL_OUT7	EN_AGC	ENABLE	RX_FRAME_N	RX_FRAME_P	TX_FRAME_N	FB_CLK_N	DATA_CLK_P	VSSD
H	RX1B_P	VSSA	VSSA	TNMRX	VSSA	VSSA	VSSD	P1_D11/TX_D5_N	VSSD	DATA_CLK_N	VDD_INTERFACE	
J	RX1B_N	VSSA	VDDA1P3_RX_SYNTH	SPI_DI	SPI_CLK	CLK_OUT	P1_D10/TX_D5_N	P1_D9/TX_D4_P	P1_D7/TX_D3_P	P1_D6/TX_D2_P	P1_D3/TX_D1_P	P1_D1/TX_D0_P
K	RX1C_P	VSSA	VDDA1P3_TX_SYNTH	VDDA1P3_BB	RESET	SPI_EN	P1_D8/TX_D4_N	P1_D6/TX_D3_N	P1_D4/TX_D2_N	P1_D2/TX_D1_N	P1_D0/TX_D0_N	VSSD
L	RX1C_N	VSSA	VSSA	RBIAS	AUXADC	SPI_DO	VSSA	VSSA	VSSA	VSSA	VSSA	VSSA
M	RX1A_P	RX1A_N	DNC	VSSA	TX_MON1	VSSA	TX1A_P	TX1A_N	TX1B_P	TX1B_N	DNC	XTALN

Legend:

- ANALOG I/O
- DC POWER
- DIGITAL I/O
- GROUND
- DO NOT CONNECT

10558-002

M12 | I | XTALN | Reference Frequency Connection. Connect the external clock source to XTALN.

¹ I is input, NC is not connected, GND is ground, O is output, P is power, and I/O is input/output.

Figure 10: Pin Layout (AD9363 (Rev. C))

3.2.1.1.G Overall Hardware Architecture

Overall, the following figure depicts the standard SDR receiver architecture that our GNSS front-end should follow:

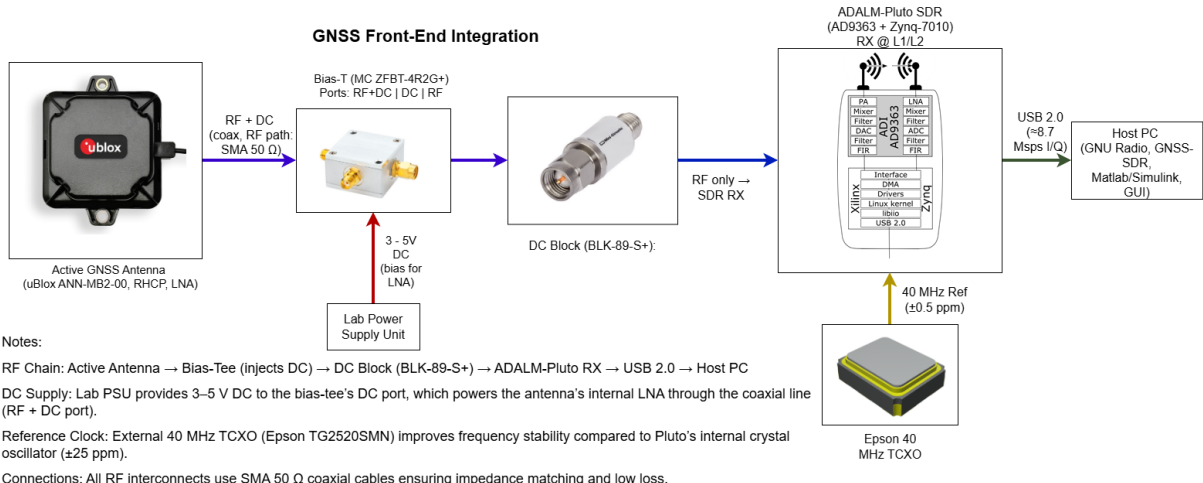


Figure 11: GNSS front-end Integration

3.2.1.1.H Hardware focused Risks and Mitigation

The following table summarizes the risks associated with the initial Hardware setup and testing phase, their corresponding impacts and possible mitigation solutions:

Table 9: Hardware focused Risks, Impacts and Mitigation solutions

Risk	Impact	Mitigation
LO drift or thermal instability	Loss of carrier/code lock	TCXO upgrade, periodic calibration
Low C/N ₀ due to cable loss or multipath	Acquisition failure	Short coax, outdoor placement, ground-plane mounting
DC leakage into SDR	Permanent hardware damage	DC block and bias-tee isolation
USB throughput bottleneck	Packet loss > 4 MSPS	Project requirement restricted to GPS L1/L2 bands
Antenna power failure	No reception	Current monitoring at bias-tee DC port
Interference in urban field	False acquisition peaks	SAW filtering and controlled test locations

3.2.1.2 Acquisition Method in GNSS Signal Processing

The acquisition process is the first functional stage of a Global Navigation Satellite System (GNSS) receiver. Its main purpose is to detect which satellites are currently visible and to determine their approximate code phase and Doppler frequency. These parameters are required to synchronize the locally generated replica signal with the incoming satellite transmission. Acquisition operates as a search procedure over possible time delays and frequency offsets that result from satellite motion, receiver dynamics, and clock differences. Successful acquisition ensures that the receiver can proceed to the tracking stage, where finer synchronization and continuous signal monitoring occur.

Because acquisition directly affects both sensitivity and Time to First Fix (TTFF), many algorithms have been proposed to optimize its performance. The classical method is based on direct correlation, where the received signal is compared with locally generated pseudorandom (PRN) codes for each satellite. However, this method is computationally demanding, so more efficient techniques such as Fast Fourier Transform (FFT)-based correlation have been developed to evaluate all code delays in parallel. Advanced implementations further reduce complexity by using methods such as circular correlation, serial and parallel code-phase search, and optimization filters like Comb or Cascaded Integrator-Comb (CIC) filters. In addition, modern multi-frequency and multi-constellation receivers perform acquisition across several signal bands simultaneously to improve robustness and speed.

Therefore, the acquisition process in GNSS can be viewed as a sequential chain of operations: first defining the delay-Doppler search space, then applying correlation through either time-domain or frequency-domain methods, and finally optimizing detection by thresholding and resource-efficient filtering. The following sections describe each of these methodological steps in detail, outlining how they collectively form the foundation of signal detection in contemporary GNSS receivers.

3.2.1.2.A Signal Reception and Sampling

The acquisition process begins with receiving and digitizing the weak GNSS signals transmitted by multiple satellites. These signals contain a carrier, a pseudorandom (PRN) code, and navigation data, and they arrive at Earth with very low power, around -160 dBW. The receiver first amplifies and down-converts them to a manageable intermediate frequency (IF) using a low-noise front end [11].

After filtering out unwanted noise, the analog signal is sampled by an analog-to-digital converter (ADC) to create a stream of digital data, often represented in I/Q format. These samples contain the complete satellite information, but with unknown code delay and Doppler frequency values. [11]

This stage provides the digital input required for acquisition algorithms. The next section focuses on forming the delay–Doppler search space, where the receiver tests various time and frequency hypotheses to identify and align with the incoming satellite signals.

3.2.1.2.B Delay–Doppler Search Space Formation

Once the GNSS signal is digitized, the receiver must identify two unknown parameters that define its alignment: the code delay and the Doppler frequency shift. These parameters determine how much the incoming signal is delayed in time and shifted in frequency compared to the locally generated replica. To estimate them, the receiver constructs a delay–Doppler search space, a two-dimensional grid containing all possible combinations of code delay and Doppler hypotheses .

Each cell in this grid represents one hypothesis pair. The receiver evaluates the correlation between the incoming signal and a locally generated replica for each cell. A strong correlation peak indicates the correct alignment, meaning the signal from a specific satellite has been successfully detected. The horizontal axis of the grid corresponds to possible code delays (τ), and the vertical axis represents Doppler frequencies (f_D). The resolution of this grid depends on the integration time, sampling frequency, and the expected Doppler range. Smaller bin sizes increase accuracy but also raise computational cost .

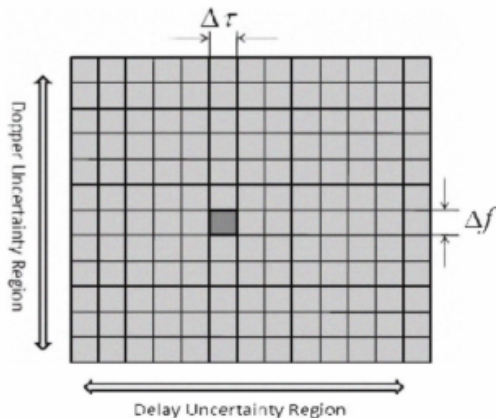


Figure 12: Two-Dimensional Search Space of Delay and Doppler Frequency [11]

The figure illustrates the delay–Doppler plane explored during acquisition. Each square (bin) represents one unique combination of code delay and Doppler frequency. The central darker cell marks the correct correlation peak where the receiver’s local code and carrier align with the incoming signal. The figure shows how increasing the number of bins improves detection precision at the cost of higher computational complexity.

Once the grid is defined, the receiver evaluates how well the incoming signal matches the locally generated replicas for all combinations of delay and Doppler. This matching process is achieved through correlation, which measures the similarity between the two signals at each point in the search grid. The correlation values across all cells form a surface where the highest peak corresponds to the correct delay and Doppler pair. To compute these values efficiently, GNSS receivers adopt structured correlation techniques that reuse signal samples within each code period. This leads naturally to the use of circular correlation, which provides an effective way to calculate all alignments across one complete code cycle without repeating unnecessary computations. The next section focuses on how circular correlation is implemented and how it forms the mathematical foundation for acquisition processing.

The most direct realization of circular correlation in hardware is the serial search acquisition method. In this scheme, each point of the delay–Doppler grid is checked sequentially, making it simple but computationally expensive. The serial search process multiplies the received IF signal with a locally generated carrier and PRN code replica for each hypothesized delay and Doppler frequency. The in-phase (I) and quadrature (Q) components are then integrated over one code period, squared, summed, and compared with a detection threshold. If the correlation amplitude exceeds the threshold, the satellite is declared acquired [11].

This method provides an intuitive time-domain interpretation of acquisition: the receiver “slides” the local replica step by step, both in frequency and code phase. Although robust and easy to implement on hardware platforms, its main drawback lies in the large computational burden, especially when thousands of code–frequency combinations must be tested. Consequently, the acquisition time becomes significantly long for multi-satellite systems, which is why frequency-domain implementations such as FFT-based circular correlation are preferred in modern receivers, offering faster processing while maintaining detection accuracy [12].

3.2.1.2.C FFT-Based Acquisition in the Frequency Domain

The computational complexity of circular and serial correlation in the time domain makes them inefficient for real-time GNSS signal processing. To overcome this limitation, modern receivers employ the Fast Fourier Transform (FFT), which allows the correlation to be calculated in the frequency domain instead of the time domain. The convolution theorem provides the theoretical basis for this approach, stating that correlation in the time domain is equivalent to multiplication in the frequency domain. This means that by transforming both the received signal and the locally generated code into the frequency domain, correlation can be achieved more efficiently through spectral multiplication followed by an inverse FFT [13].

In the FFT-based approach, the incoming digitized intermediate-frequency (IF) signal $y_{IF}(n)$ and the locally generated code $y_c(n)$ are first transformed using FFT:

$$Z(k) = Y_c(k) \cdot Y(k)_{IF}^*$$

where $Y_{IF}^*(k)$ and $Y_c(k)$ denote the FFTs of the received and local signals. Since taking conjugate in frequency domain means time reversal in the time domain circular correlation is equal to multiplying Y_c and conjugate of Y_{IF} .

The time-domain correlation result is then recovered using the inverse FFT (IFFT):

$$z(n) = IFFT\{Z(k)\}$$

The peak of $|z(n)|$ identifies the correct code delay and Doppler frequency, completing the acquisition process [13].

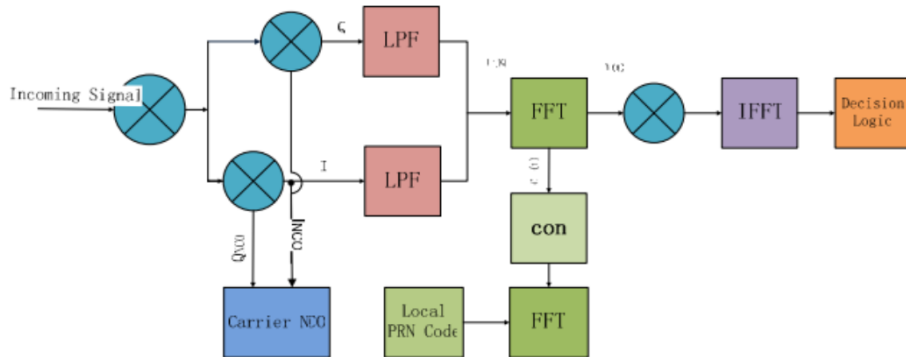


Figure 13: FFT-Based Circular Correlation Block Diagram [13]

FFT-based acquisition reduces computational complexity from the order of N^2 in the serial search to the Order of $N \log \log N$ in the frequency domain. This allows real-time acquisition even for long PRN sequences and multiple satellites. In addition, FFT-based approaches reuse the same processing modules for both FFT and IFFT. FFT-based model gets rid of the calculation burden of τ , but it cannot get rid of the Doppler frequency calculation.

To acquire multiple satellites or frequency bands, modern receivers perform FFT-based correlation across several Doppler bins in parallel. Each Doppler bin corresponds to a frequency offset hypothesis that is removed by pre-mixing the IF signal before FFT processing. The resulting two-dimensional correlation surface provides the maximum likelihood estimate of both delay and frequency.

3.2.1.2.D Optimization Techniques (Comb, Multi-Frequency)

The process of simultaneously utilizing GNSS signals provided on various frequency bands, such as GPS L1 C/A, L2C, and L5, to increase the acquisition

stage's speed, sensitivity, and resilience is known as multi-frequency acquisition. Each satellite in a modern GNSS constellation (such as GPS, Galileo, and BeiDou) broadcasts numerous signals, each of which is scaled according to carrier frequency but experiences the same underlying satellite-to-receiver dynamics, particularly Doppler shift and code delay. By utilizing these common characteristics, multi-frequency acquisition greatly narrows the search space and enhances detection efficiency [14]. Since the Doppler shift is proportional to the signal's carrier frequency, once Doppler is estimated on one frequency, the Doppler search window on other frequencies can be reduced to a very narrow interval. This reduces the computational load [14]. Multi-frequency approaches can combine signals in two ways, which are noncoherent and coherent combining [14]. Phase-aligned signals from different frequencies are combined before correlation.

3.2.1.2.E Detection and Decision

The receiver must determine whether a correlation peak represents a real satellite signal or only noise after the acquisition stage calculates the correlation values over all code phases and Doppler bins. A binary hypothesis test is used to formulate this decision-making process. The null hypothesis is there is noise only (no satellite present), and the alternative hypothesis is there is signal plus noise (satellite present). For each Doppler bin, the maximum correlation value is extracted, and the global peak P is selected. Then the corresponding $(\tau, f_{D'})$ represent the estimated code delay and Doppler [15]. For many receivers, it is common to normalize the metrics. It should be checked whether it meets the threshold criteria. The threshold is chosen to satisfy the false alarm probability [16]. If the detection criteria is satisfied, the receiver states that the satellite acquired and transmits the estimated code delay and Doppler to the tracking loops (DLL/PLL/FLL). If not, the search proceeds and the PRN is marked as absent.

This phase directly affects sensitivity and time-to-first-fix (TTFF) by guaranteeing accurate satellite detection and preventing spurious acquisitions [17]. In addition to the previous discussion, the following table details the acquisition focused risks and the respective mitigation strategies.

Table 10: Acquisition focused Risks, Impacts and Mitigation solutions

Risk	Impact	Mitigation
False acquisition due to noise or multipath interference.	Faulty, misleading acquisition may slow the navigation chain.	Apply adaptive detection threshold, cross-correlation validation.

The subsequent sections fall later in our work timeline for the project so they are briefly discussed.

3.2.1.3 Tracking Method in GNSS Signal Processing

The tracking process ensures accurate Doppler frequency shift and the code phase shift due to relative velocities of the receiver and the satellite. The tracking process is planned to be achieved by using DLL (delay locked loop) for PRN code phase lock, and a FLL (frequency locked loop) for the carrier frequency lock regarding GPS L1 and L2 signal structure. The following table details the tracking focused risks and the respective mitigation strategies.

Table 11: Tracking focused Risks, Impacts and Mitigation solutions

Risk	Impact	Mitigation
Loss of lock under low CNR conditions.	Telemetry decoding fails.	Efficient signal conditioning, digital filtering can be used to improve performance.

3.2.1.4 Telemetry Decoding and Data Processing

When the tracking loop ensures the lock on the satellite signal, the base-band signal is decoded for acquiring the navigation data from the satellite. This process involves frame synchronization, parity checking, and data extraction for observable, clock corrections, and gathering almanac information. The following table details the telemetry focused risks and the respective mitigation strategies.

Table 12 : Telemetry decoding focused Risks, Impacts and Mitigation solutions

Risk	Impact	Mitigation
Bit error due to clock jitters or loss of synchronization.	Loss of observable data.	Error checking (parity check, soft decision decoding) can be regarded.

3.2.1.5 PVT Computation

The PVT solver stage of GNSS signal processing generates estimates for position, velocity, and time solutions, given at least four satellites' observables from

navigation data. The following table details the PVT computation focused risks and the respective mitigation strategies.

Table 13 : PVT algorithm focused Risks, Impacts and Mitigation solutions

Risk	Impact	Mitigation
Numerical instability or inconsistent observables	Faulty PVT solutions outputted in the GUI.	Use hybrid observables and perform cross-checking for outliers

3.2.1.6 GUI Design and System Integration

The GUI Design and System Integration phase focuses on combining all GNSS processing modules - acquisition, tracking, telemetry decoding, and PVT into a single functional workflow and providing a simple interface for real-time visualization. Since this is the final stage of the project and depends on earlier modules being fully validated, the current work mainly involves defining the GUI structure and establishing data connections with GNSS-SDR rather than implementing the full interface. The planned GUI will be developed in Python and will visualize key system outputs such as estimated C/N₀ values, the number of tracked satellites, a basic satellite skyplot, and the receiver's computed position at 1 Hz, in accordance with GUI-R-1 to GUI-R-4. The following table details the GUI focused risks and the respective mitigation strategies.

Table 14: GUI focused Risks, Impacts and Mitigation solutions

Risk	Impact	Mitigation
Data format mismatch between GNSS-SDR and GUI	Incorrect C/N ₀ or satellite display	Standardize output format (JSON/CSV)
GUI refresh delay or slow rendering	Lag in constellation/position updates	Use lightweight plotting and 1 Hz updates

GUI crash under unexpected values (e.g., 0 satellites)	Loss of visualization	Add basic exception handling
--	-----------------------	------------------------------

3.2.2 Progress and the current state

The following figures illustrates an attempt from our side to simulate certain algorithms discussed in previous section on already available raw data:

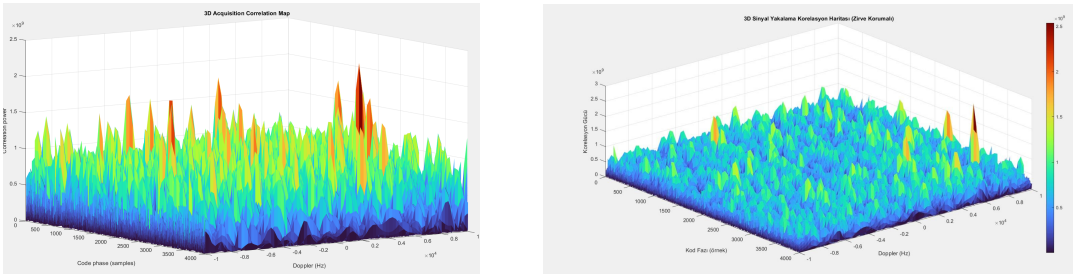


Figure 14: PCPS algorithm simulations on MATLAB with pre-recorded data.

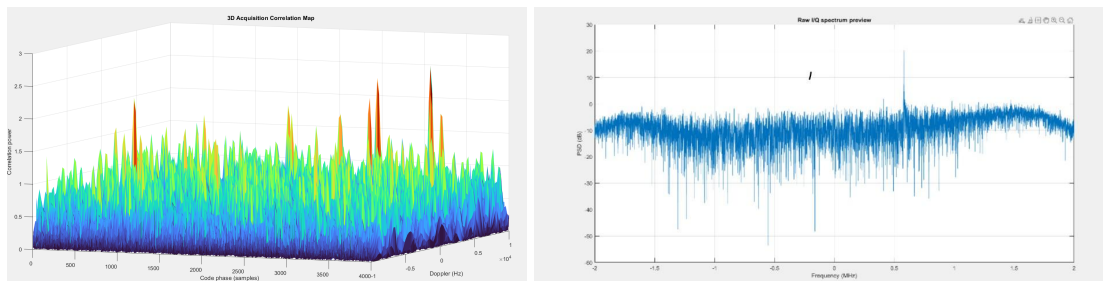


Figure 15: Generated PCPS plot and PSD analysis of pre-recorded data



Figure 16: Generated PVT Solutions using GNSS SDR.

The recent progress of the project can be explained in terms of literature review on SDR devices, geolocation/navigation methodologies, GNSS signal structures and processing, and specifically GPS L1 and L2 signal structures and signal processing chains. The GNU Radio software and GNSS SDR software were set up and started to be used. Additionally, MATLAB simulations over acquisition

were performed using pre-recorded baseband data, whose results are shown in the figures above. The following figure summarizes our progress upto now:

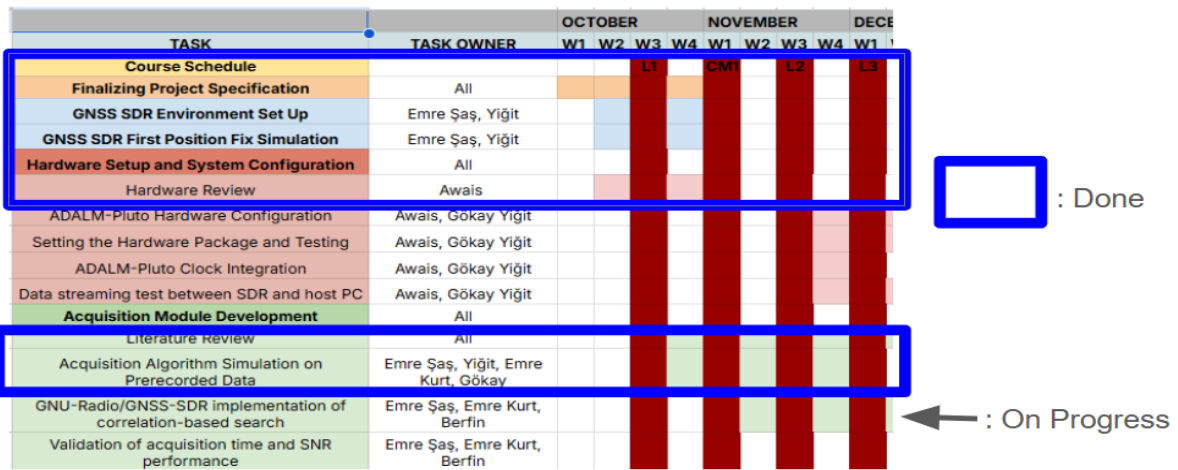


Figure 17: Progress upto now (14.11.2025) on Gantt Chart

4. DETAILED EQUIPMENT LIST

Table 15: Detailed equipment list and costs

Product	Price (USD)	Way To Obtain
ADI Adalm Pluto SDR REV C	233	By Purchase
U-blox ANN-MB2-00	66.95	By Purchase
Mini-Circuits ZFBT-4R2G+ Bias Tee	80.60	By Purchase
Mini-Circuits BLK-89-S+	20.26	By Purchase
Epson TG2520SMN Temperature-Compensated Crystal Oscillator	5	By Purchase
Total Price	405.81	

5. REFERENCES

- [1] European Space Agency (ESA), *Navipedia Main Page*. ESA GSSC Navipedia, 2025. [Online]. Available: https://gssc.esa.int/navipedia/index.php/Main_Page [Accessed: 13 Nov. 2025].
- [2] Analog Devices, Inc., *ADALM-PLUTO SDR Active Learning Module—Product Highlight*, Rev. A, Norwood, MA, USA, 2017. [Online]. Available: <https://www.analog.com/en/design-center/evaluation-hardware-and-software/evaluation-boards-kits/adalm-pluto.html>
- [3] Huace Microelectronics (HMuSRP), *Products*. [Online]. Available: https://www.hmusrp.com/products/?gad_source=1&gad_campaignid=21734890059 [Accessed: 28 Sep. 2025].
- [4] B. M. Ledvina, M. L. Psiaki, S. P. Powell, and P. M. Kintner, Jr., “Real-time software receiver,” U.S. Patent 7,010,060, Mar. 7, 2006.
- [5] B. M. Ledvina, M. L. Psiaki, S. P. Powell, and P. M. Kintner, Jr., “Real-time software receiver,” U.S. Patent 7,305,021, Dec. 4, 2007.
- [6] K. Van Dierendonck, M. Xu, and P. L. Kazemi, “System, method, and computer program for a low power and low cost GNSS receiver,” U.S. Patent 9,116,234, Aug. 25, 2015.
- [7] u-blox AG, *ANN-MB2 L1/L2/L5/E6/B3/L All-Band High-Precision GNSS Antenna—Data Sheet*, Document UBX-DOC-963802114-12775, Thalwil, Switzerland, Feb. 2025. [Online]. Available: <https://www.u-blox.com/en/product/ann-mb-series>
- [8] Mini-Circuits, *ZFBT-4R2G+ Coaxial Bias-Tee (10–4200 MHz)*, Data Sheet, Rev. D, Brooklyn, NY, USA, 2024. [Online]. Available: <https://www.minicircuits.com/WebStore/dashboard.html?model=ZFBT-4R2G%2B>
- [9] Mini-Circuits, *BLK-89-S+ Coaxial DC Block (0.1–8000 MHz)*, Data Sheet, Rev. G, Brooklyn, NY, USA, 2024. [Online]. Available: <https://www.minicircuits.com/WebStore/dashboard.html?model=BLK-89-S%2B>
- [10] Seiko Epson Corporation, *TG2520SMN Temperature-Compensated Crystal Oscillator (TCXO) Full Data Sheet*, Spec. No. TG2016/2520SMN_EN Ver. 2.0, Tokyo, Japan, 2025. [Online]. Available: <https://www.epsondevice.com/crystal/en/products/crystal-oscillator/tg2520smn.html>
- [11] R. Khan, S. U. Khan, R. Zaheer, and S. Khan, “Acquisition strategies of GNSS receiver,” in *Proc. Int. Conf. Computer Networks and Information Technology (ICCNIT)*, Jul. 2011, pp. 119–124, doi: 10.1109/ICCNIT.2011.6020917.
- [12] Y. Li, Q. Zhao, C. He, and J. Hu, “Optimization of GNSS signals acquisition algorithm complexity using comb decimation filter,” in *Proc. IEEE Int. Conf.*

Computer Science, Artificial Intelligence and Electronic Engineering (CSAIEE), 2021, pp. 268–272, doi: 10.1109/CSAIEE54046.2021.9543328.

- [13] Q. Lei and L. Lei, “GPS signal acquisition based on FFT,” in *Proc. 2nd Int. Conf. Information Technology and Computer Science (ITCS)*, 2010, pp. 110–113, doi: 10.1109/ITCS.2010.33.
- [14] S. Cui, D. Wang, B. Holtkamp, X. Yao, T. Chi, and J. Fang, “A multi-frequency acquisition algorithm for a GNSS software receiver,” in *Proc. IEEE Int. Geosci. Remote Sens. Symp. (IGARSS)*, Jul. 2018, doi: 10.1109/IGARSS.2018.8517898.
- [15] M. Foucras, B. Ekambi, F. Bacard, O. Julien, and C. Macabiau, “Assessing the performance of GNSS signal acquisition: new signals and GPS L1 C/A code,” *Inside GNSS*, Jul./Aug. 2014, pp. 68–76. [Online]. Available: <https://insidegnss.com/assessing-the-performance-of-gnss-signal-acquisition/>. [Accessed: 13 Nov. 2025].
- [16] A. Albu-Rghaif, H. Y. Radhi, and R. G. Dawood, “Combining GPS and Galileo signals acquisition in a single processing chain,” *Diyala Journal of Engineering Sciences*, pp. 157–167, Dec. 2024, doi: 10.24237/djes.2024.17409.
- [17] M. Andrianarison and G. Macabiau, “New approach of high-sensitivity techniques using GNSS mass-market receivers,” *Sensors*, vol. 18, no. 11, 3690, 2018, doi: 10.3390/s18113690.